Accuracy Assessment of a Phase Domain Line Model

Martin G. Vega, J. L. Naredo, O. Ramos-Leaños

Abstract--**The Phase-Domain Line Model, or Universal Line Model (ULM), is among the most advanced ones for time-domain analysis of EMTs in power lines and cables. This model must perform two convolutions, one involving the characteristic admittance matrix function $\mathbb{Y}_c$ and the other the transfer-function matrix for traveling waves of currents $\mathbb{H}$. To perform these convolutions recursively, both matrices must be fitted rationally. In the case of matrix $\mathbb{H}$, previous identification and extraction of the travel-time factors is required. The impact of the various stages of the model build-up and execution on the final accuracy is assessed here by means of the Numerical Laplace Transform (NLT) technique. It is reported here that the major accuracy loss is related to the matrix-$\mathbb{H}$ convolutions and particularly to the proper identification of the line travel-times. A non-iterative method based on the NLT is proposed here for travel-time identification.**

Keywords: **Electromagnetic transients, time delays, impulse response, compensation, ULM, Laplace, NLT.**

I. INTRODUCTION

Electromagnetic transient (EMT) analysis and simulation of power systems often requires accurate models of power transmission lines and cables. Nowadays the Phase-Domain Line Model, also known as the Universal Line Model (ULM) [1], is perhaps the most advanced and used of its class. This model is based on the principle of traveling waves and its implementation in EMTP-type programs requires the numeric evaluation of two convolution processes, one that involves the characteristic admittance matrix $\mathbb{Y}_c$ of the line and the other involving the line transfer matrix-function $\mathbb{H}$ for the traveling waves of currents [1,2].

To perform the required convolutions in a numerically efficient manner, matrices $\mathbb{Y}_c$ and $\mathbb{H}$ must be first approximated by rational functions (or polynomial matrices) [3]. This usually is accomplished with the Vector Fitting (VF) utility [6]. The rational approximation of $\mathbb{H}$ requires, in addition, the previous identification of the characteristic travel-times of the line and the subsequent extraction of their related delay-factors from the elements of $\mathbb{H}$.

Once the rational representations of $\mathbb{Y}_c$ and $\mathbb{H}$ are obtained, the associated convolutions can be conveniently represented in state-space as sets of ordinary differential equations (ODEs). For their solution inside ULM, these ODEs are subsequently converted into difference equations through the application of a numerical integration rule which for both, the EMTP and the ULM, usually is the trapezoidal rule [2].

This paper is concerned with the numerical accuracy of EMT simulations of lines and cables through the ULM; that is, under the assumption of $\mathbb{Z}$ and $\mathbb{Y}$ line matrices being accurate, what is the numeric error level introduced by the ULM in the simulated time-domain transient waveforms? To answer this, a commercial grade implementation of the ULM is compared against a frequency-domain line model which is solved through the Numerical Laplace Transform (NLT) technique [5,14,15]. The latter technique has the advantage of its numerical accuracy being well-determined and amenable of being controlled to a large extent. For the purposes of this paper, the accuracy of the NLT-based line model is tuned to an accuracy of 10^{-9}; that is, the relative error-level. This is accomplished using a number of $N=2^{19}$ (524 288) samples for both, the time and the frequency ranges [5]. The comparison between the NLT and the EMTP-ULM models shows that the accuracy of the latter is in the order of 10^{-2}; that is, about 1 % accuracy. It is thus considered here that this level must be improved further.

Subsequent analysis is performed in this paper using the NLT technique to pin-down the major source of error in the ULM. The following aspects are analyzed here: 1) rational fit of $\mathbb{Y}_c$, 2) identification of line travel-times, 3) rational fit of $\mathbb{H}$ and 4) numerical integration of the convolution related ODEs. It is found here that the major loss of accuracy in the ULM is on the identification of the line travel-times and that this also has a bad impact on the accuracy of the rationally fitted $\mathbb{H}$ matrix.

Previous to this paper, it has been reported at reference [7] that the identified and extracted travel-times have an impact on the accuracy of the fitting of $\mathbb{H}$. An iterative method based on Brent´s optimization is thus introduced in [7] to determine the travel-time values that minimize the *rms* error in the fit of $\mathbb{H}$ by VF. In this paper a new methodology is introduced to compensate an initial travel-time estimate to a value that increases substantially the accuracy of ULM-generated transient waveforms. This methodology is based on the NLT technique and a major advantage upon the one based on Brent´s method is that it is non-iterative. When applied to the EMTP-ULM, the new methodology results in an accuracy increase of the time domain responses from 10^{-2} to almost 10^{-4}. Mention is made here to the fact that, with respect to the travel-time obtained with Brent´s method, the one determined with the new methodology not always results in better fits for $\mathbb{H}$ (i.e., lower VF defined *rms* errors); nevertheless, it usually results in more accurate time-domain transient responses.

Martín G. Vega is with the Electrical Engineering Department, Cinvestav, Guadalajara 45019, México (e-mail: mvega@gdl.cinvestav.mx).

J. L. Naredo is with the Electrical Engineering Department, Cinvestav, Guadalajara 45019, México (e-mail: jlnaredo@gdl.cinvestav.mx).

O. Ramos-Leaños is with Safe Engineering Services & technologies ltd., Laval, QC,H7L 6E8, Canada (e-mail: octavio.ramos.leanos@gmail.com)

II. THE PHASE-DOMAIN LINE MODEL

A. Model Equations

As most power-line models for EMT analysis, the ULM is based on the following frequency-domain form of the Telegrapher Equations:

$$\frac{d\mathbb{V}}{dx} = -\mathbb{Z}\mathbb{I} \quad \text{and} \quad \frac{d\mathbb{I}}{dx} = -\mathbb{Y}\mathbb{V} \tag{1}$$

where $\mathbb{V}$ and $\mathbb{I}$ are the respective vectors of voltage and current phasors along the line conductors, $\mathbb{Z}$ and $\mathbb{Y}$ are the respective matrices of series impedances and of shunt admittances, both in per unit length. These two matrices are of order $N_c{\times}N_c$ for a line with N_c independent conductors.

Given a line-segment of length "l", as the one depicted in Fig. 1a, the solution of (1) in terms of traveling waves of currents is expressed as follows [1,2]:

$$\mathbb{I}_0 = \mathbb{Y}_c\mathbb{V}_0 - \mathbb{H}[\mathbb{I}_l + \mathbb{Y}_c\mathbb{V}_l] \tag{2}$$
$$\mathbb{I}_l = \mathbb{Y}_c\mathbb{V}_l - \mathbb{H}[\mathbb{I}_0 + \mathbb{Y}_c\mathbb{V}_0] \tag{3}$$

with sub-indexes "0" and "l" indicating the values of vectors $\mathbb{V}$ and $\mathbb{I}$ the respective segment-ends $x = 0$ and $x = l$. $\mathbb{Y}_c$ and $\mathbb{H}$ are the respective matrices of characteristic admittances and of propagation transfer-functions for the traveling waves of currents [1,2]:

$$\mathbb{Y}_c = \sqrt{\mathbb{Y}\mathbb{Z}}\,\mathbb{Z}^{-1} = \Gamma\,\mathbb{Z}^{-1} \tag{4}$$

$$\mathbb{H} = e^{-\sqrt{\mathbb{Y}\mathbb{Z}}l} = e^{-\Gamma l}. \tag{5}$$

One way to rewrite (2) which is more convenient in the ULM context is as follows [2]:

$$\mathbb{I}_0 = \mathbb{I}_{sh,0} - \mathbb{I}_{aux,0} \tag{6}$$

with

$$\mathbb{I}_{sh,0} = \mathbb{Y}_c\mathbb{V}_0 \tag{7}$$
$$\mathbb{I}_{aux,0} = \mathbb{H}\mathbb{I}_{rfl,l} \tag{8}$$
$$\mathbb{I}_{rfl,l} = \mathbb{I}_l + \mathbb{Y}_c\mathbb{V}_l \tag{9}$$

where $\mathbb{I}_{rfl,l}$ is the vector of currents being reflected at terminal "l". An equivalent expression for (3) in the form of (6) is obtained by exchanging sub-indexes "0" and "l" in relations (6) to (9). Expressions (2) and (3) lead to the circuit model depicted in Fig. 1b for the line segment under consideration.

The ULM requires the representation of matrices $\mathbb{Y}_c$ and $\mathbb{H}$ by rational (or polynomial) forms. The rational approximation of $\mathbb{Y}_c$ is as follows [1,2]:

$$\mathbb{Y}_c \cong \mathbb{G}_0 + \sum_{k=1}^{N_y} \frac{\mathbb{G}_k}{s - p_k} \tag{10}$$

where N_y is the order of the rational approximation, p_k is the $k-th$ pole, $\mathbb{G}_k$ is the $k-th$ matrix of residues associated to p_k and $\mathbb{G}_0$ is a matrix of constants obtained as the limit of $\mathbb{Y}_c$ when $s \rightarrow \infty$. The poles of $\mathbb{Y}_c$ are determined from its trace.
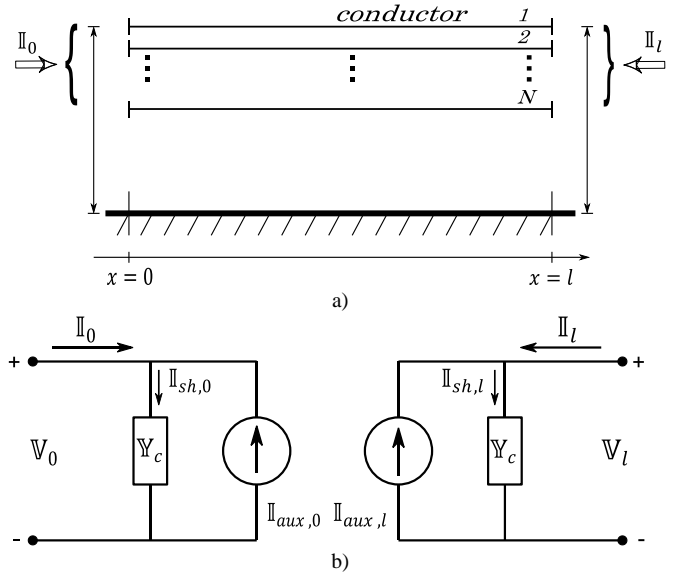

Fig. 1.a) Multiconductor Transmission Line-Segment, b) Equivalent circuit in the frequency domain for the line-segment.

The rational approximation of $\mathbb{H}$ is more elaborate than the one of $\mathbb{Y}_c$. The reason being that all the elements in $\mathbb{H}$ contain combinations of all modal-delay factors of the line. It is thus necessary to decouple and to extract every single delay as follows [7]:

$$\mathbb{H} = \sum_{i=1}^{N_m} \mathbb{H}_i \cong \sum_{i=1}^{N_m} \left[\sum_{k=1}^{N_{h,i}} \frac{\mathbb{R}_{i,k}}{s - q_{i,k}} \right] e^{-s\tau_i} \tag{11}$$

where N_m also corresponds to the number of propagation modes in the line and $N_{h,i}$ indicates the order of the rational-approximation for the $i-th$ mode (eigenvector), $q_{i,k}$ is the $k-th$ pole for the $i-th$ mode, $\mathbb{R}_{i,k}$ is the matrix of residues corresponding to the $q_{i,k}$ pole, τ_i is the travel-time of the $i-th$ mode. The technique used in the rational synthesis of $\mathbb{Y}_c$ and $\mathbb{H}$ is Vector Fitting (VF) [6]. The term $\mathbb{H}_i$ in (11) corresponds to the propagation function for the $i-th$ mode and, for its rational fitting, it can be determined from (5) through modal analysis methods. Details of this are given in [2].

B. Model Equations

Frequency-domain expressions (7) and (8) correspond in time-domain to the convolution terms to be performed by the ULM. Their state-space representation is obtained by first introducing (10) and (11) into (7) and (8) as follows:

$$\mathbb{I}_{sh} = \mathbb{G}_0\mathbb{V} + \sum_{k=1}^{N_y} \mathbb{W}_k; \;\; \mathbb{W}_k = \frac{\mathbb{G}_k}{s - p_k}\mathbb{V} \tag{12}$$

$$\mathbb{I}_{aux} = \sum_{i=1}^{N_m} \sum_{k=1}^{N_{h,i}} \mathbb{X}_{i,k}; \; \mathbb{X}_{i,k} = \frac{\mathbb{R}_{i,k}e^{-s\tau_i}}{s - q_{i,k}}\mathbb{I}_{rfl} \tag{13}$$

Then, by applying the inverse Laplace transform in (12)

and (13):

$$\mathbb{i}_{sh} = \mathbb{G}_0 \mathbb{v} + \sum_{k=1}^{N_y} \mathbb{w}_k ; \qquad \frac{d\mathbb{w}_k}{dt} = p_k \mathbb{w}_k + \mathbb{G}_k \mathbb{v} \tag{14}$$

$$\mathbb{i}_{aux} = \sum_{i=1}^{N_m} \sum_{k=1}^{N_{h,i}} \mathbb{x}_{i,k} ; \qquad \frac{d\mathbb{x}_{i,k}}{dt} = q_{i,k} \mathbb{x}_{i,k} + \mathbb{R}_{i,k} \mathbb{i}'_{rfl} \tag{15}$$

Note that sub-indexes 0 and l have been omitted in expressions (12)-(13), as well as in (14) and (15). This is to keep mathematical notation simple. The expressions (14) and (5) are the basis for the ULM and correspond to two set of ODEs.

III. FREQUENCY DOMAIN LINE MODEL

The line segment at Fig. 1a can be considered as a two-port network with the following nodal representation [8, 9]:

$$\begin{bmatrix} \mathbb{I}_0 \\ \mathbb{I}_l \end{bmatrix} = \begin{bmatrix} \mathbb{A} & \mathbb{B} \\ \mathbb{B} & \mathbb{A} \end{bmatrix} \begin{bmatrix} \mathbb{V}_0 \\ \mathbb{V}_l \end{bmatrix} \tag{16}$$

where

$$\mathbb{A} = \cosh(\mathbb{T}l)\mathbb{Y}_c, \tag{17}$$
$$\mathbb{B} = -\operatorname{csch}(\mathbb{T}l)\mathbb{Y}_c. \tag{18}$$

For the purposes of this paper, expressions (16)-(18) are related as follows to the line representation at (2) and (3) that is in terms of the $\mathbb{Y}_c$ and $\mathbb{H}$ matrices [10]:

$$\begin{bmatrix} \mathbb{I}_0 \\ \mathbb{I}_l \end{bmatrix} = \begin{bmatrix} \mathbb{Y}_{11} & \mathbb{Y}_{12} \\ \mathbb{Y}_{21} & \mathbb{Y}_{22} \end{bmatrix} \begin{bmatrix} \mathbb{V}_0 \\ \mathbb{V}_l \end{bmatrix} \tag{19}$$

with

$$\mathbb{Y}_{11} = \mathbb{Y}_{22} = (\mathbb{U} - \mathbb{H}^2)^{-1}(\mathbb{H}^2 + \mathbb{U})\mathbb{Y}_c \tag{20}$$
$$\mathbb{Y}_{12} = \mathbb{Y}_{21} = (\mathbb{U} - \mathbb{H}^2)^{-1}(-2\mathbb{H})\mathbb{Y}_c. \tag{21}$$

IV. TIME DELAY IDENTIFICATION

Accurate rational approximations require that fitted functions are of minimum phase. Transfer matrix function $\mathbb{H}$ is not minimum phase since it includes all the line-mode delays $\tau_1, \tau_2, \dots, \tau_{N_c}$. These delays must thus be identified and extracted from the $\mathbb{H}$ matrix by expressing it as follows:

$$\mathbb{H} = \sum_{i=1}^{N_m} \widehat{\mathbb{H}}_i e^{-s\tau_i} \cong \sum_{i=1}^{N_m} e^{-s\tau_i} \sum_{k=1}^{N_{h,i}} \frac{\mathbb{R}_{i,k}}{s - q_{i,k}} . \tag{22}$$

Comparing (11) and (22) it follows that

$$\mathbb{H}_i = \widehat{\mathbb{H}}_i e^{-s\tau_i} \tag{23}$$

and $\widehat{\mathbb{H}}_i$ is minimum phase matrix function. It is thus clear that the terms $\widehat{\mathbb{H}}_i$ are the ones to be fitted rationally. Let $H_i = H_i(\omega)$ denote any nonzero element of $\mathbb{H}_i$. According to Bode's formula, for a minimum phase function the magnitude $|H_i|$ and its phase $\varphi_i(\omega)$ are related as follows:

$$\varphi_i(\omega) = \frac{\pi}{2} \frac{d(\ln|H_i(\omega)|)}{d(\ln \omega)} \bigg|_{\omega = \Omega_i} + \Delta_i(\omega) \tag{24}$$

with

$$\Delta_i(\omega) = \frac{1}{\pi} \int_{-\infty}^{+\infty} \left(\left| \frac{d(\ln|H_i|)}{du_i} \right| - \left| \frac{d(\ln|H_i|)}{du_i} \right|_{u=0} \right) \ln\left(\coth \frac{|u_i|}{2} \right) du_i \tag{25}$$

and

$$u_i = \ln \frac{\Omega_i}{\omega} \tag{26}$$

Ω_i above corresponds to the frequency at which $|H_i| = 0.1|H_i(\omega)||_{\omega=0}$. The phase angle at this frecuency provides a good estimate as follows for the $i - th$ modal-delay to be extracted from $\mathbb{H}_i$ [4]:

$$\tau_i = \frac{l}{v_i(\Omega_i)} + \frac{\varphi_i}{\Omega_i} \tag{27}$$

here v_i is the $i - th$ mode velocity and l is the transmission line-length.

V. TEST CASES

Consider a single phase transmission line being connected as it is shown in Fig. 2. Table I provides the line dimensions, as well as its electric properties. At $x = 0$ the line is connected to an ideal voltage source that injects a voltage unit step and at $x = l$ the line is open-circuited. The line transient response at $x = l$ is first obtained with the NLT using 524 288 frequency samples to attain a numeric accuracy of 10^{-9}. This transient response is plotted in Fig. 3 and it is adopted here as the reference to evaluate the results obtained from four other tests that are described next.
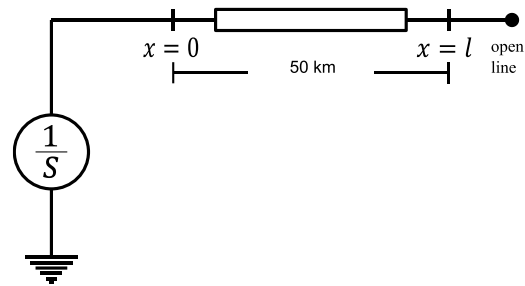

Fig. 2. Transmission line connections.

TABLE I

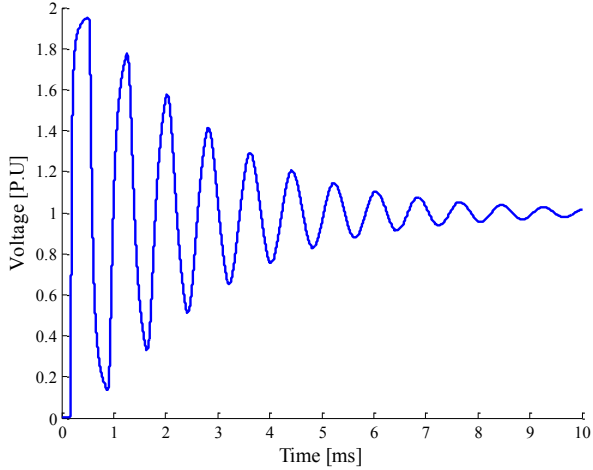| Line Data	
Line length	50 km
Conductor height	10 m
Nr. of phases	1
Conductor radius	0.0158 m
Nr. of condutors in bundle	2
Bundle radius	0.20 m
Conductors resistivity	3.21e-8 Ω-m
Ground resistivity	100 ohm-m
Ground relative permittivity	1

Fig. 3. Transient response obtained with the NLT.

Fig. 4. Error level for the EMTP-ULM transient response.

A. Test Nr. 1

This test consists in obtaining the transient waveform at $x = l$ for the line connection depicted in Fig. 2 by means of the ULM in EMTP-RV, as well as in its comparison with the NLT results. Figure 4 provides a plot for the relative errors of the EMTP-ULM waveform where one can observe that the error level is around 10^{-2}.

B. Test Nr. 2

Now, the transient response of the line depicted at Fig. 2 is obtained again through the NLT technique. However, this time the analytic expression of $\mathbb{Y}_c$ at (4) is replaced by its rational approximation obtained with VF as in expression (10). The transient response so obtained is compared against the reference one at Fig. 3. The plot of relative differences between these two responses is provided in Fig. 5. Note from this figure that the difference level is below 10^{-14}. One can thus conclude that the rational approximation of $\mathbb{Y}_c$ has nil effect on the overall accuracy of the ULM.

C. Test Nr. 3

This test consists in obtaining the transient response of the line in Fig. 2 again with the NLT. This time now, only the analytic expression for $\mathbb{H}$ as in expression (5) is replaced by its rational fit as in (11). This rational fit, along with the estimated travel-time, is as provided by the EMTP-ULM . The transient waveform so obtained is compared with the reference one in Fig. 3. Figure 6 provides the error plot for the waveform obtained with fitted $\mathbb{H}$. Note that the error level is around the 10^{-2} figure which is similar to the one in Fig. 4. One can thus conclude from this result that the accuracy loss in the EMTP-ULM is mostly due to the rational approximation of $\mathbb{H}$, along with the estimated line travel-time.

D. Test Nr. 4

The final test consists in obtaining the transient response for the line at Fig. 2 through the NLT technique with rational approximations for both, $\mathbb{Y}_c$ and $\mathbb{H}$. The transient waveform being obtained is now compared with the one from the EMTP-ULM as in Test Nr. 1. Figure 7 provides the relative hat the
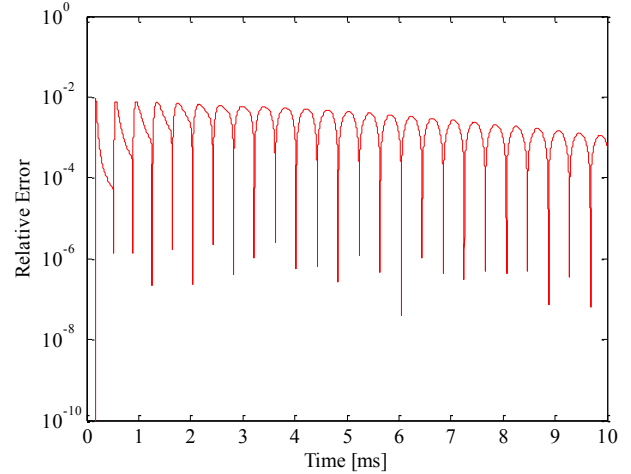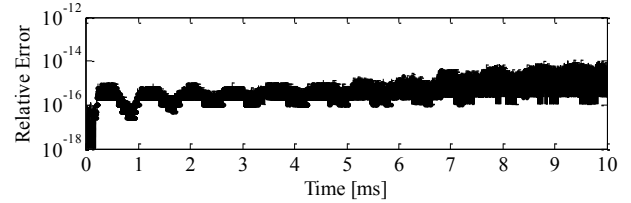

Fig. 5. Differences between the reference waveform and the one obtained with NLT and the rational fit of $\mathbb{Y}_c$.
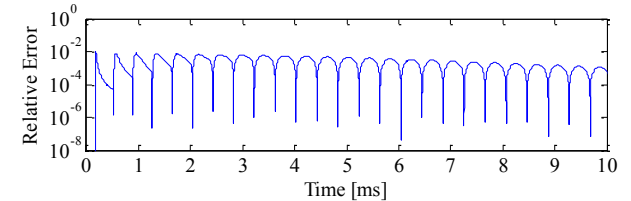

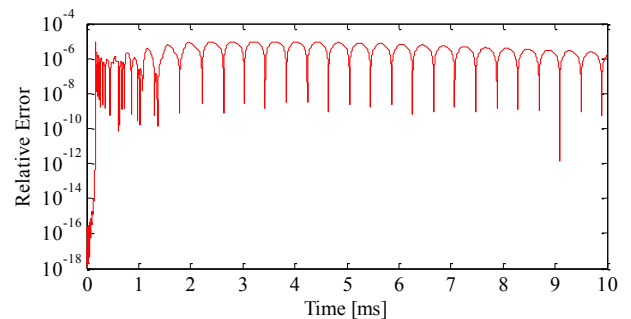Fig. 6. Error level corresponding to the application of rationally fitted $\mathbb{H}$.

Fig. 7. Relative differences between transient waveforms obtained with EMTP-ULM and NLT with rational fits of $\mathbb{Y}_c$ and $\mathbb{H}$.

difference level is in the order of 10^{-6} (i.e., one millionth). One can thus conclude that the accuracy loss in the EMTP-ULM has been replicated with the NLT-based line model. One can also conclude from this result that the accuracy loss due to the numeric integration of the state-space ODEs is nil too.

VI. COMPENSATING TRAVEL-TIME ESTIMATES

The estimation of line travel-times is essential to attain an accurate fit of the $\mathbb{H}$ transfer matrix. Figure 8 shows for instance the rational fit of $\mathbb{H}$ obtained for the single-phase line at section V under two different travel-time estimates: τ_0 and τ_1. The first one is obtained with the conventional method applying expression (27). The second one has been obtained here by a trial-and-error process. Figure 8 illustrates the fact that a rational approximation of $\mathbb{H}$ being based on the conventional travel-time estimate τ_0 from (27) is not optimal. According to the figure, the one based on $\tau_1 > \tau_0$ actually is more accurate. Table II provides the *rms* errors in the rational adjustments of $\mathbb{H}$ based on the travel-time estimates τ_0 and τ_1.
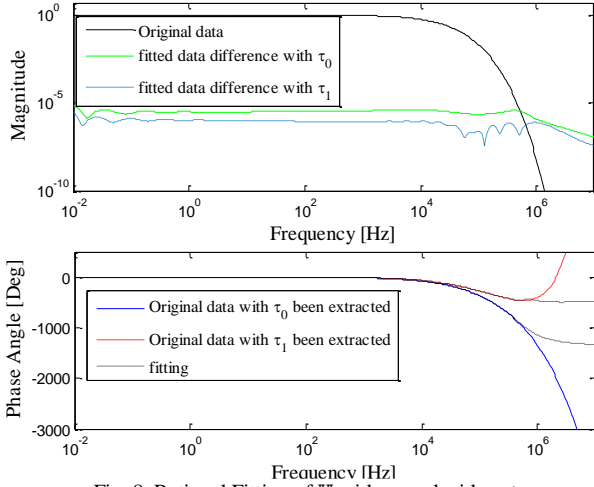

Fig. 8. Rational Fitting of $\mathbb{H}$ with τ_0 and with $\tau_1 > \tau_0$

TABLE I

Time Delays		
τ	$\tau_0=1.668419367360679e-4$	$\tau_1=1.693489792999174e-4$
$\mathcal{E}_{rms}$	2.983357406488400e-6	8.594404292141444e-7

A more convenient alternative to the trial-and-error process previously used for the determination of τ_1 is the systematic method proposed at reference [7]. This is an iterative process based on Brent's optimizatio n method that searches for the travel-time estimate that minimizes the *rms* error level at the rational approximation of $\mathbb{H}$. Another non-iterative method is proposed here next. This new method aims at reducing the error in the time-domain transient response of the line model and it is based on the NLT technique.

It is well-known that if a transfer function in the "*s*" frequency-domain, say $H(s)$, represents a time-invariant linear system, its inverse Laplace transform yields the system's impulse response $h(t)$:

$$H(s) \xrightarrow{\mathcal{L}^{-1}} h(t)$$

Let τ_0 be a first estimate of a line travel-time being obtained perhaps by (27), and let $\widehat{\mathbb{H}}$ represent the line propagation function with the travel time τ_0 being extracted as follows:

$$\widehat{\mathbb{H}} = \mathbb{H}e^{\tau_0 s}$$

Now, a rational approximation of $\widehat{\mathbb{H}}$ is obtained through VF as $\widehat{\mathbb{H}}_{fit}$. Figure 9 shows the impulse responses derived from

applying the inverse NLT to both functions $\widehat{\mathbb{H}}$ and $\widehat{\mathbb{H}}_{fit}$. One can observe at this figure that the impulse response obtained from $\widehat{\mathbb{H}}_{fit}$ has been delayed slightly with respect to the one from $\widehat{\mathbb{H}}$. This is a side-effect from the rational fitting process which should be compensated to decrease numeric errors with the convolution processes related to the line $\mathbb{H}$ matrix. The time compensation-term, being denoted here as τ', could be obtained in principle as the time difference between the maximum values of the two impulse responses. Nevertheless, it should be considered that the impulse responses, by being obtained through the NLT, are time-discretized and their resolution is limited. Nevertheless, to obtain a better estimate of the compensation term the resolution of the impulse responses can be increased through an interpolation process. Here, the maximum sampled value of each impulse is first detected; then, each maximum point is used along with its four closest sample points to produce a fourth order polynomial. The time difference between the two polynomial maxima provides a better estimate for the needed compensation time. Figure 9 also includes the impulse response obtained from $\widehat{\mathbb{H}}_{EMTP}$; that is,the rational approximation of $\widehat{\mathbb{H}}$ obtained from the EMTP-ULM.

Travel-time estimate τ_0 is thus compensated by adding the previously determined term τ':

$$\tau_1 = \tau_0 + \tau'. \tag{28}$$

The new travel-time value τ_1 is further used to obtain a better rational approximation $\widehat{\mathbb{H}}_{fit}$. Figure 10 shows the new impulse-response plot from $\widehat{\mathbb{H}}_{fit}$. As the new values of τ_1 and $\widehat{\mathbb{H}}_{fit}$ are applied with the ULM, the accuracy of its transient responses is increased. Figure 11 provides the relative error plot for the Test Nr. 4 from section V as the new values of τ_1 and of $\widehat{\mathbb{H}}_{fit}$ are used with the EMTP-ULM. Note that the error plots for Test Nr. 1 (EMTP-ULM without delay compensation) are also included in this figure from comparison purposes. The comparison shows that the technique being proposed here increases the numeric accuracy-level of the ULM in more than an order of magnitude.
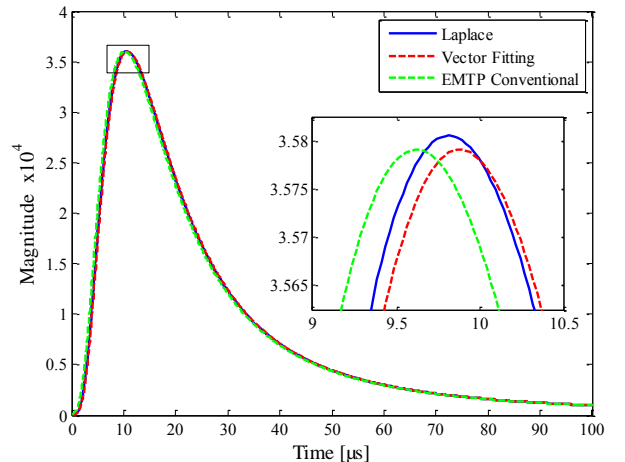

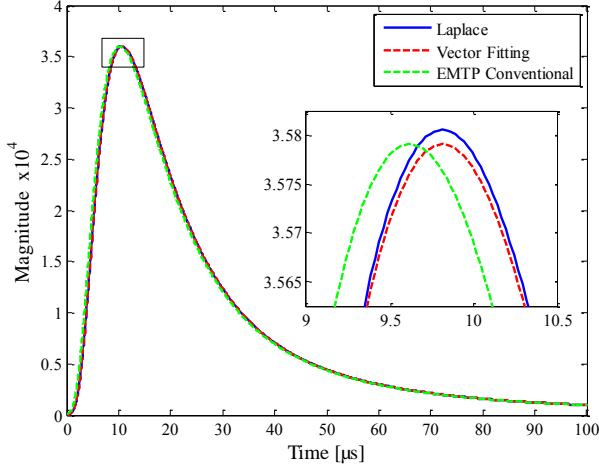Fig. 9. Impulse response with uncompensated τ_0

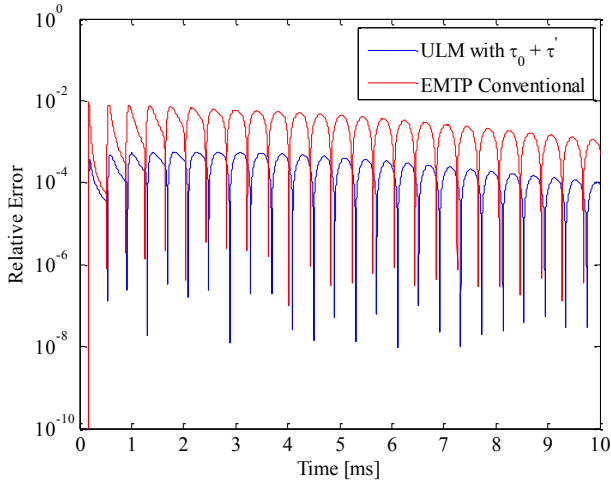Fig. 10. Impulse response with compensated $\tau_1 = \tau_0 + \tau'$

Fig. 11. Improvement in the overall error-level of the ULM by the proposed compensation technique.

VII. CONCLUSIONS

The numerical accuracy of the phase-domain line model (ULM) has been evaluated in this paper by means of the Numerical Laplace Transform technique. For this purpose, the NLT has been tuned-up for an accuracy of 10^{-9}. This has required the use of a number of $N=2^{19}$ samples in both, the time-domain and the frequency-domain range. Evaluation of commercial-grade implementations of the ULM has been performed by comparing its time-domain transient responses with those obtained from the NLT technique. Although the ULM version used in this study is the one in EMTP-RV version 2.5, similar results have been obtained with the one in PSCAD-EMTDC.

First, it has been found that the overall numerical accuracy of the ULM is around 10^{-2}. Then, the following four aspects of the ULM implementation have been evaluated in terms of their impact on the accuracy of the ULM time-domain results: 1) the rational fit of $\mathbb{Y}_c$, 2) the identification of line travel-times, 3) the rational fit of $\mathbb{H}$ and 4) the numerical integration of the convolution related ODEs. This analysis has shown that both, the rational fit of $\mathbb{Y}_c$ and the numerical integration of the state-space ODEs do not have practically a negative impact on

the accuracy of the ULM. In fact, the major loss in accuracy has been found to be associated to the identification of line travel-times. In addition, their proper identification is crucial to attain an accurate rational fit of matrix $\mathbb{H}$.

The standard method to identify line travel-times is by a heuristic method based on a formula by Bode that relates magnitude and phase for minimum-phase transfer functions [7]. Travel-times obtained with this method can be refined further as proposed in [7] through an iterative method based on Brent's optimization; this is used to decrease the VF-defined *rms* error in the rational approximation of $\mathbb{H}$. As an alternative, a non-iterative method has been proposed in this paper to compensate first approximations of travel-times. This new method is based on the NLT technique and it has been found here that, when applied to the ULM, the so obtained compensated travel-times result in an accuracy increase of the time domain transient responses from 10^{-2} to almost 10^{-4}. Even though these results are encouraging, these authors consider that further research still is needed to improve the overall accuracy of the ULM.

VIII. APPENDIX

EMT analysis in time-domain involves the operations of integration, differentiation and convolution. An advantage achieved in frequency-domain is that these operations become algebraic. If $X(s)$ is the Laplace transform of $x(t)$ [5]

$$X(s) = \int_0^\infty x(t)e^{-st}dt. \qquad (29)$$

The inverse Laplace transform is defined as [5, 14]

$$x(t) = \frac{1}{2\pi}\int_{c-\infty}^{c+\infty} X(s)\, e^{st}ds. \qquad (30)$$

A numerical approximation of (30) is as follows [5, 14]:

$$x(n) = \frac{e^{cn\Delta t}}{\Delta t}\left\{\frac{1}{N}\sum_{m=0}^{N-1} X_m e^{2\pi jmn/N}\right\} \qquad (31)$$

where N is the number of samples used to describe $X(s)$;

$$X_m = X(c + jm\Delta\Omega),$$

$$x(n) = x(n\Delta t)$$

and

$$\Delta\Omega = \frac{2\pi}{N\Delta t}$$

note that the term into a brackets in (31) is the discrete Fourier transform (DFT) of X_m [12], this is evaluated directly by the Fast Fourier transform algorithm (FFT). Therefore (31) can be expressed by:

$$x(n) = \frac{e^{cn\Delta t}}{\Delta t} ifft\{[X(c + jm\Delta\Omega) \times \sigma_m(m\Delta\Omega)]_{m=0}^{N-1}\} \qquad (32)$$

where σ_m is a window function used to decrease the error known as Gibbs'; This error is inflicted by the truncation of the integral in (30) [12]. Aliasing error minimization is attained here by a proper choice of damping coefficient "c". This coefficient is calculated as follows [5]:

$$c = -[log_e(\epsilon_{rel})]/T \qquad (33)$$

where T is the maximums observation time of the transient and ϵ_{rel} is the targeted relative error. Wedepohl reports in [15] that the ϵ_{rel} can be calculated by the following relation

$$\epsilon_{rel} = 1/N^b, \qquad 1 < b < 2. \qquad (34)$$

This criterion has been determined by a trial-and-error process.

IX. References

[1] A. Morched, B. Gustavsen, and M. Tartibi, "A universal model for accurate calculation of electromagnetic transients on overhead lines and underground cables", *IEEE Trans. on Power Delivery,* vol. 14, no. 3, pp. 1032-1038, July 1999.

[2] Octavio Ramos-Leaños, Jose Luis Naredo and Jose Alberto Gutierrez-Robles. "An Advanced Transmission Line and Cable Model in Matlab for the Simulation of Power-System Transients" in *MATLAB - A Fundamental Tool for Scientific Computing and Engineering Applications*, 1st ed., Volume 1, Prof. Vasilios Katsikis, Ed. InTech Open, ISBN: 978-953-51-0750-7, DOI: 10.5772/48530. Available from: http://www.intechopen.com/books/matlab-a-fundamental-tool-for-scientific-computing-and-engineering-applications-volume-1/an-advanced-transmission-line-and-cable-model-in-matlab-for-the-simulation-of-power-system-transient.

[3] Semlyen, A.; Dabuleanu, A., "Fast and accurate switching transient calculations on transmission lines with ground return using recursive convolutions,"*Power Apparatus and Systems, IEEE Transactions on* , vol.94, no.2, pp.561,571, Mar 1975.

[4] Gustavsen, B.; Semlyen, A., "Simulation of transmission line transients using vector fitting and modal decomposition,"*Power Delivery, IEEE Transactions on* , vol.13, no.2, pp.605,614, Apr 1998.

[5] Jose L. Naredo, Jean Mahseredjian, Ilhan Kocar, José A. Gutiérrez–Robles, Juan A. Martinez–Velasco, "Frequency Domain Aspects of Electromagnetic Transient Analysis of Power Systems" in *Transient Analysis of Power Systems: Solution Techniques, Tools and Applications*, 1st ed., vol. 1. Juan A. Martinez-Velasco, Ed. New York: IEEE-John Willey, 2015, pp. 39-70. ISBN 9781118352342.

[6] Gustavsen, B.; Semlyen, A., "Rational approximation of frequency domain responses by vector fitting,"*Power Delivery, IEEE Transactions on* , vol.14, no.3, pp.1052,1061, Jul 1999.

[7] L. De Tommasi and B. Gustavsen,"Accurate transmission line modeling through optimal time delay identification". In *Proc. Int. Conf. on Power Systems Transients, IPST, 2007.*

[8] L. M. Wedepohl,"Theory of natural modes in multiconductor transmission lines" in *Lecture Notes for Course ELEC-552*, The University of British Columbia, 1982.

[9] L. Wedepohl and R. Wasley, "Propagation of carrier signals in homogeneous, nonhomogeneous and mixed multiconductors systems," *Electrical Engineers, Proceedings of the Institution of,* vol. 115, no. 1, pp. 179-186, 1968.

[10] Semlyen, A.; Gustavsen, B., "Phase-Domain Transmission-Line Modeling With Enforcement of Symmetry Via The Propagated Characteristic Admittance Matrix," *Power Delivery, IEEE Transactions on* , vol.27, no.2, pp.626,631, April 2012

[11] H. W. Bode, *Network analysis and feedback amplifier design.* Van Nostrand Reinhold, 1956.

[12] J. G. Proakis and D. G. Manolakis, *Digital Signal Processing. Principles, Algorithms and Applications*, Prentice-Hall, 4th Edition, 2007.

[13] B. P. Lathi, *Linear Systems and Signals*, Berkeley Cambridge Press, 1992.

[14] Moreno, P.; Ramirez, A., *"Implementation of the Numerical Laplace Transform: A Review Task Force on Frequency Domain Methods for EMT Studies, Working Group on Modeling and Analysis of System Transients Using Digital Simulation, General Systems Subcommittee, IEEE Power Engineering Society,"* Power Delivery, IEEE Transactions on , vol.23, no.4, pp.2599,2609, Oct. 2008.

[15] L. M. Wedepohl, *"Power system transients: Errors Incurred in the Numerical Inversion of the Laplace Transform".*Proc. of the twenty-sixth Midwest Symposium on Circuits and Systems, pp. 174-178, August 1983.